Science in China Series D: Earth Sciences

© 2009 SCIENCE IN CHINA PRESS
Springer

www.scichina.com
earth.scichina.com
www.springerlink.com

V_p and V_p/V_s structures in the crust and upper mantle of the Taiwan region, China

LI ZhiWei†, XU Yi, HAO TianYao & XU Ya

Key Laboratory of Petroleum Resources Research, Institute of Geology and Geophysics Chinese Academy of Sciences, Beijing 100029, China

A tomographic study of the V_p and V_p/V_s structures in the crust and upper mantle beneath the Taiwan region of China is conducted by simultaneous inversion of P and S arrival times. Compared with the previous tomographic results, the spherical finite difference technique is suitable for the strong heterogeneous velocity structure, and may improve the accuracy in the travel time and three-dimensional ray tracing calculations. The V_p and V_p/V_s structures derived from joint inversion and the relocated earthquakes can provide better constraints for analyzing the lateral heterogeneity and deep tectonic characters in the crust and upper mantle. Our tomographic results reveal significant relations between the seismic wavespeed structure and the tectonic characters. In the shallow depth, sedimentary basins and orogen show distinct wavespeed anomalies, with low V_p, high V_p/V_s in basins and high V_p, low V_p/V_s in orogen. As the suture zone of Eurasian Plate and Philippine Sea Plate, Longitudinal Valley is characterized by a significant high V_p/V_s anomaly extending to the middle-lower crust and upper mantle, which reflects the impact of rock cracking, partial melting, and the presence of fluids. In the northeast Taiwan, the V_p, V_p/V_s anomalies and relocated earthquakes depict the subducting Philippine Sea Plate under the Eurasian Plate. The high V_p of oceanic plate and the low V_p, high V_p/V_s atop the subducted oceanic plate extend to 80 km depth. Along the east-west profiles, the thickness of crust reaches 60 km at the east of Central Range with eastward dipping trend, which reveals the eastward subduction of the thickened and deformed crust of the Eurasian continental plate.

Taiwan region, P wave velocity, V_p/V_s ratio, lithosphere structure, tomography

Taiwan region of China is located in the collision belt between the Eurasian Plate and the Philippine Sea Plate, and becomes a natural laboratory for the study of mountain building, arc-continent collision, and subduction[1−3] (Figure 1). The western Coastal Plain, Western Foothills, Central Range, Longitudinal Valley are located across the Taiwan island from the west to the east, and the crust thickness varies greatly, which is about 20−35 km at the western Coastal Plain, and up to 55 km at the Central Range. To the Longitudinal Valley and Coastal Range area, the crust turns to be oceanic type, and the thickness decreases rapidly[4,5]. The main tectonic units and seismicity spread in NNE-SSW direction, parallel to the collision frontier of Eurasian Plate and Luzon volcanic arc. The geological processes in the northeast Taiwan are related to the subducting of the Philippine Sea oceanic plate along the Ryukyu trench.

The previous studies indicated that the Philippine Sea Plate is moving northwestward at a velocity of 7−8 cm/a relative to the Eurasian Plate, which results in the oblique collision between Luzon Arc and Eurasian Plate and the forming of Taiwan orogen[6−8]. The main arc-

Received June 10, 2008; accepted February 19, 2009
doi: 10.1007/s11430-009-0091-2
†Corresponding author (email: zwli@mail.iggcas.ac.cn)
Supported by Knowledge Innovation Program of the Chinese Academy of Sciences (Grant No. KZCX3-SW-234-2), National Basic Research Program of China (Grant No. 2007CB411701), National High Technology Research and Development Program of China (Grant No. 2006AA09A101-0201) and National Natural Science Foundation of China (Grant Nos. 40804016, 40704013)

Citation: Li Z W, Xu Y, Hao T Y, et al. V_p and V_p/V_s structures in the crust and upper mantle of the Taiwan region, China. Sci China Ser D-Earth Sci, 2009, 52(7): 975-983, doi: 10.1007/s11430-009-0091-2

continent collision process occurred near the Longitudinal Valley spanning 22°—23.5°N, where there is the suture zone of the Eurasian and Philippine Sea Plates[9,10]. Except in the Hualien region, the collision and deformation are not very obvious[11]. However, as the key place of subduction mechanism transform, Hualien region exhibits the complex tectonics and deep dynamic process involving two different subduction styles: in the northeast of Taiwan area, the Philippine Sea Plate is underthrusting the Eurasian Plate along the Ryukyu trench; while in the southeast, the Eurasian Plate is underthrusting the Philippine Sea Plate[2,4,5,12—14]. Collision and subduction are responsible for crust deforming and thickening, mountain building, and active seismicity. Seismological studies suggest that the deformation is not only limited in the middle-upper crust, but also extends to the lower crust and upper mantle[4,5,9,15,16].

The dense network of seismic stations and the large amount of arrival time observations make it possible to study the velocity structures in the crust and upper mantle. Based on the previous tomographic results, Roecker et al.[17] showed the evidence of the different underthrusting relations between the Eurasian Plate and the Philippine Sea Plate in the north and south of Taiwan island. Rau et al.[4] identified the subducted slab of the Philippine Sea Plate under the Eurasian Plate dipping at an angle of 40º to the depth of 100—130 km in the north of Taiwan, and provided strong evidence for the involvement of crust and upper mantle in the arc-continent collision and mountain building. Kim et al.[5] analyzed the relations between earthquake activity and deep tectonics in the crust and upper mantle. Wang et al.[13] showed the 65—80 km thick high velocity lithosphere of the Eurasian Plate underthrusting the Philippine Sea Plate down to a depth of 300 km. Wu et al.[18] revealed the main tectonic units and deep characters of the arc-continent collision zone.

The V_p/V_s ratio is an important parameter for analyzing the petrology and rheology of the crust and upper mantle, and could provide more constraints than V_p or V_s. In this study, we adopt the spherical finite difference technique to implement the seismic travel time and three-dimensional ray tracing computation, which is suitable for the strongly heterogeneous velocity structure of the crust and upper mantle in Taiwan region[19,20]. The V_p and V_p/V_s ratio structures in the crust and upper mantle are simultaneously determined using the local and regional P and S first arrival times jointly.

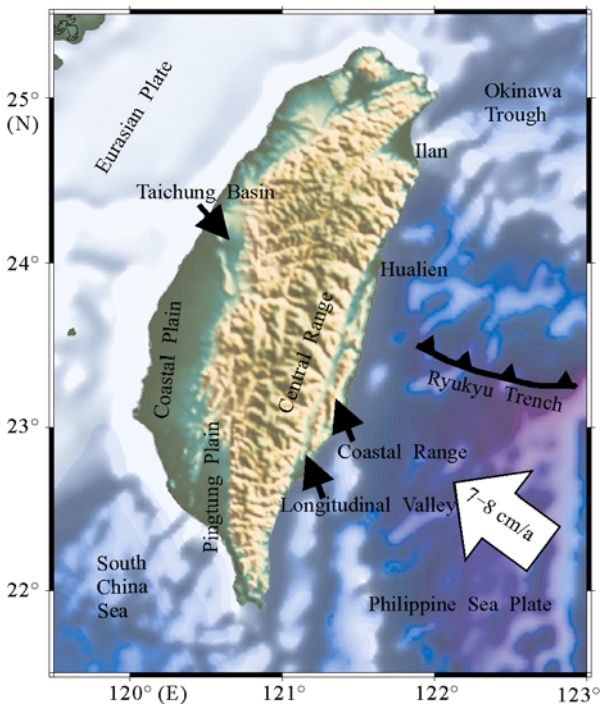

Figure 1 The tectonic framework of the Taiwan region.

1 Method and data

1.1 Method

As a later-arrival seismic wave, S-wave arrivals are not as clear as the first P-wave arrivals, and the picking uncertainty of S-wave is also much greater than the P wave, therefore the quantity of S-wave data is also less than the P-wave. Because of these reasons, the S-wave velocity structure derived from S-wave arrival times also has greater uncertainty than P-wave structure[21,22], and the V_p/V_s directly calculated from V_p and V_s will have too great uncertainty for tectonic analyses. So, we invert for the V_p and V_p/V_s structures simultaneously rather than for V_p and V_s separately in this study[23].

The P-wave travel time residual δt_{ij}^{p} can be represented by

$$\delta t_{ij}^{\mathrm{p}} = t_{ij}^{\mathrm{obs}} - t_{ij}^{\mathrm{cal}} = \sum \frac{\partial t}{\partial S_k^{\mathrm{p}}} \Delta S_k^{\mathrm{p}} + \sum_{l=1}^{4} \frac{\partial t}{\partial q_l^i} \Delta q_l^i, \qquad (1)$$

where t_{ij}^{obs} is the observed travel time from the ith earthquake to the jth station, t_{ij}^{cal} is the synthetic travel time calculated from model, S_k^{p} is the P-wave slowness at the kth grid point in model, q_l^i (l=1, 2, 3, 4)are the source parameters of the ith earthquake (including

focal depth, latitude, longitude, and origin time). Similarly, the S-wave travel time residual δt_{ij}^{s} can be represented by

$$\delta t_{ij}^{s} = t_{ij}^{obs} - t_{ij}^{cal} = \sum \frac{\partial t}{\partial S_k^s} \Delta S_k^s + \sum_{l=1}^{4} \frac{\partial t}{\partial q_l^i} \Delta q_l^i, \quad (2)$$

where S_k^s is the S-wave slowness at the kth grid point in model. From eq. (2), we know there are no obvious relations between V_p and V_s except the same source parameters, if we implement the inversion separately for V_p and V_s. However, P- and S-wave arrival times will be influenced by some of the same factors, such as mineral composition, temperature, pressure, and pore fluid and so on, and thus the variations of V_p and V_s are not totally independent. To build the linear equations for solving V_p/V_s, with eq. (2), the V_p/V_s ratio $r_k = V_p/V_s = S_k^s / S_k^p$ at kth grid point in model can be represented as[24]

$$\sum \frac{\partial t}{\partial S_k^s} \Delta S_k^s = \sum \frac{\partial t}{\partial S_k^s} \Delta (r_k S_k^p) = \sum \frac{\partial t}{\partial S_k^s} (S_k^p \Delta r_k + r_k \Delta S_k^p). \quad (3)$$

Using eqs. (2) and (3), we can obtain the linear equations relating S travel time residual to P wave slowness, V_p/V_s ratio, and source parameters. The linear equations for solving V_p, V_p/V_s and source parameters simultaneously consist of eqs. (1)—(3).

Three-dimensional ray tracing and travel time calculation are conducted by finite difference technique in spherical rather than Cartesian coordinate system[19,20], thus avoiding the distortion of coordinate system and Earth flattening transform. Compared with the approximate ray tracing technique, the finite difference technique can improve the accuracy in strongly heterogeneous media and reduce the ambiguity in determining global travel time minima[24]. Hypocenters are determined via grid search approach, which can always find the true minimum in data variance[24]. The system of linear equations for tomographic inversion is solved using the LSQR algorithm[25]. In the linear equations, we still keep the equations for source parameters to reduce the bias to the velocity structure.

We take the previous tomographic results as the references to build the starting model[5,18], and adjust it according to the travel time residuals of the current dataset. We choose a fine grid spacing of 2 km for travel time computation and a nominal coarser grid of 10 km laterally and 4—20 km in depth (shown in Table 1) for wavespeed inversion. To improve the computation accuracy and also make it feasible, we use one-fifth fine grid spacing near the source region (within 100 km from the source)[19,20].

Table 1 Initial model of V_p and V_p/V_s ratio used in this study

Depth (km)	V_p (km·s^{-1})	V_p/V_s
0	5.10	1.73
4	5.50	1.73
10	6.00	1.73
16	6.20	1.73
22	6.40	1.73
28	6.80	1.73
36	7.60	1.73
46	7.85	1.73
60	7.95	1.73
80	8.00	1.73
100	8.04	1.73
120	8.10	1.73

1.2 Data

The P and S arrival times are from the seismic station networks in the Taiwan region during 1992—2004, which are located inside the study region of 21.5°—25.8°N and 119.5°—123.5° E. The selection of travel times is based on the following criteria: (1) the focal depth of earthquake is shallower than 100 km; (2) each earthquake is recorded by at least 6 stations with P and S arrival times; (3) travel time residuals must be inside ±4.0 s. The entire dataset consists of about 135000 P and 77000 S arrivals from nearly 6000 events recorded at 92 stations, the hypocenters and stations are shown in Figure 2.

2 Results and analysis

After three iterations, the V_p and V_p/V_s model can fit the observed arrival times very well; the root-mean-square travel time residual was reduced from 0.99 to 0.60 s.

2.1 Resolution test

We constructed the checkerboard velocity model by adding ±4% of variation to the initial model with horizontal anomaly size about 30 km×30 km at each depth. Figures 3 and 4 show the recovered V_p and V_p/V_s checkerboard results separately. Since most of the stations are located on land, the V_p and V_p/V_s structures are recovered better beneath the island to the depth 46 km. Down to the depth of 60—80 km, the recovery shows signs of

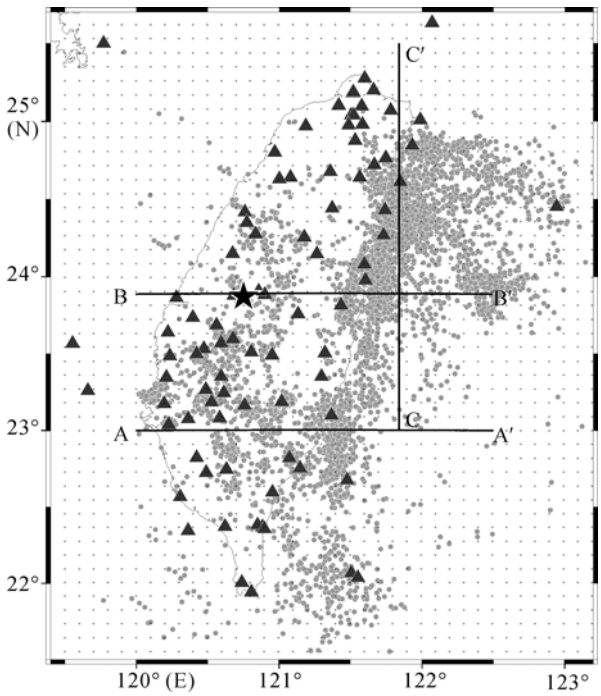

Figure 2 Station and hypocenter distributions. Triangles indicate seismic stations. Open circles show the hypocenters. The nodes of model grid are plotted as small crosses. The pentagram shows the position of M_w 7.6 Chi-Chi earthquake on September 21, 1999.

smearing because of the lack of enough ray path sampling. The recovery of V_p is also better than that of V_p/V_s, which is due to more P arrivals than S. In the end, we analyzed the deep structures of Taiwan region based on V_p and V_p/V_s results down to 80 km.

2.2 V_p and V_p/V_s structures

Figures 5 and 6 present the V_p and V_p/V_s structures at 0—80 km depth from the inversion, with the relocated hypocenters within ±10 km of each depth.

The V_p and V_p/V_s structures at 0—10 km depths reveal the tectonic characters of upper crust. The sedimentary basins in the western Coastal Plain show low V_p and high V_p/V_s anomalies, which may be related to the thick and water-saturated sediments[19,22]. High V_p and low V_p/V_s signals are consistent with the distribution of metamorphic outcrops in Central Range. High V_p/V_s anomalies at Longitudinal Valley and Coastal Range extend down to the uppermost mantle, where the velocity anomaly and hypocenter distribution depict the collision belt of Eurasian Plate and Luzon Arc. The high V_p/V_s anomaly in this suture zone may indicate the partial melting and the presence of fluids. The Philippine Sea Plate is characterized by high V_p and low V_p/V_s, which reflects the property of oceanic plate.

At 16—46 km depths, the scope of low V_p anomaly at western Coastal Plain shrinks and turns to be high V_p with the increasing of depth, the high V_p/V_s anomaly also becomes weaker. In contrast to the western Coastal Plain, the low V_p signals at Pingtung Plain in south Taiwan extend to 36 km depth, with significantly high V_p/V_s anomaly down to 28 km depth. Since the northern boundary of the Pingtung Plain is coincident with the northern edge of the Manila trench, previous studies indicated that the rapid subsidence of this basin is the surface manifestation of the subducting oceanic lithosphere prior to the collision of the fore-arc ridge and the continental margin[18,26], which is also coincident with the low V_p signals extending to middle-lower crust and upper mantle and the seismicity distributed in north-south direction. With the increasing of depth, the low V_p anomalies beneath the western Coastal Plain migrate eastward beneath the Central Range and its eastern region, which is still significant at 46 km depth and reflects the variation of crust thickness. While at the depth of 36 km beneath the eastern Coastal Range and to the eastern ocean, there is obvious high V_p strongly contrasting to the low V_p beneath the Central Range. The strong variation of V_p/V_s characters at Hualien and nearby Philippine Sea area indicates the difference between the oceanic and continental crust, which is also related to the active earthquakes.

To the depth of 60—80 km, the Central Range and the area to its east are characterized by large scale low V_p and high V_p/V_s anomalies. Previous studies indicated that the thickness of crust beneath the Central Range and eastern Taiwan reaches 50—55 km due to the collision of the Eurasian Plate and the Philippine Sea Plate[4,5,9]. The low V_p character is also related to the collision. On one hand, it indicates the underthrusting Eurasian continental plate beneath the Philippine Sea Plate. On the other hand, it suggests the existence of fluids and partial melting in the crust-mantle boundary and uppermost mantle. It is similar with the low V_p and moderate high V_p/V_s signals beneath the volcanic area in north Taiwan observed by Kim et al.[5]. These anomalies could be due to the dehydration caused by the high temperature and pressure or the fluids induced by the subducting Eurasian Plate.

2.3 V_p and V_p/V_s profiles

Profiles of V_p and V_p/V_s with relocated earthquakes are shown in Figures 7(a)—(c), depicting the crustal struc-

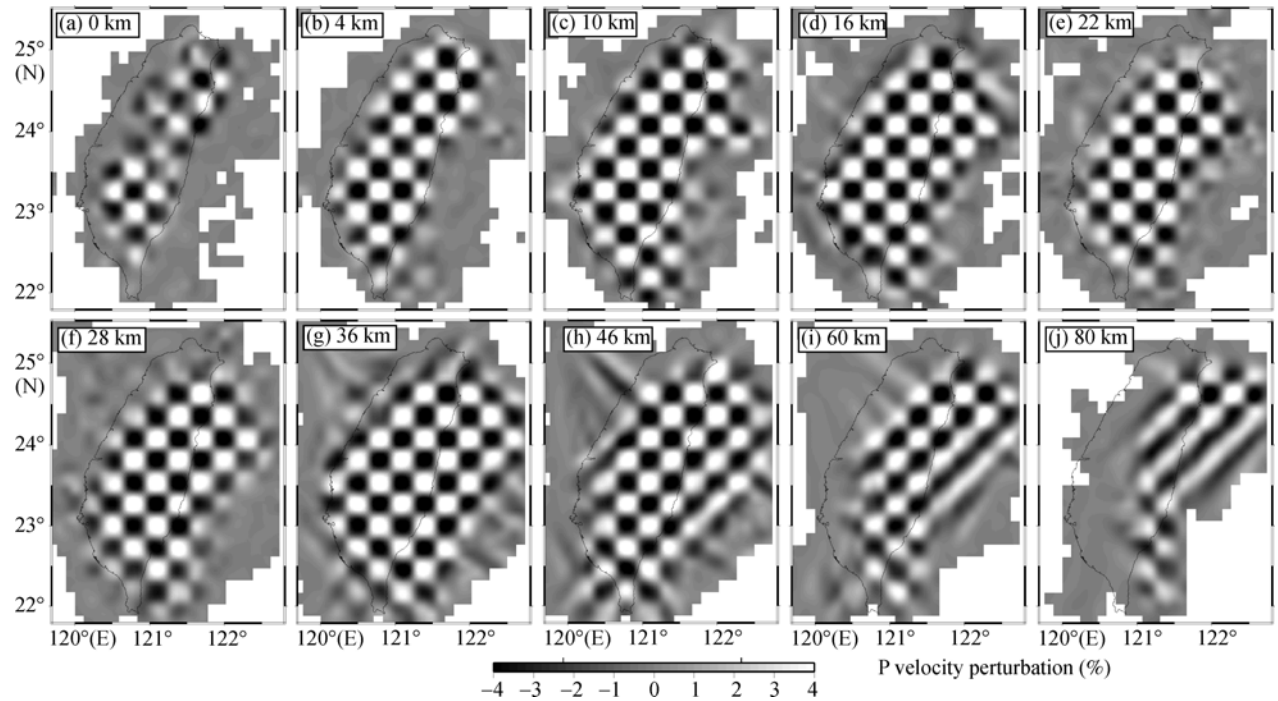

Figure 3 Recovered V_p models in checkerboard resolution tests at 0—80 km depth.

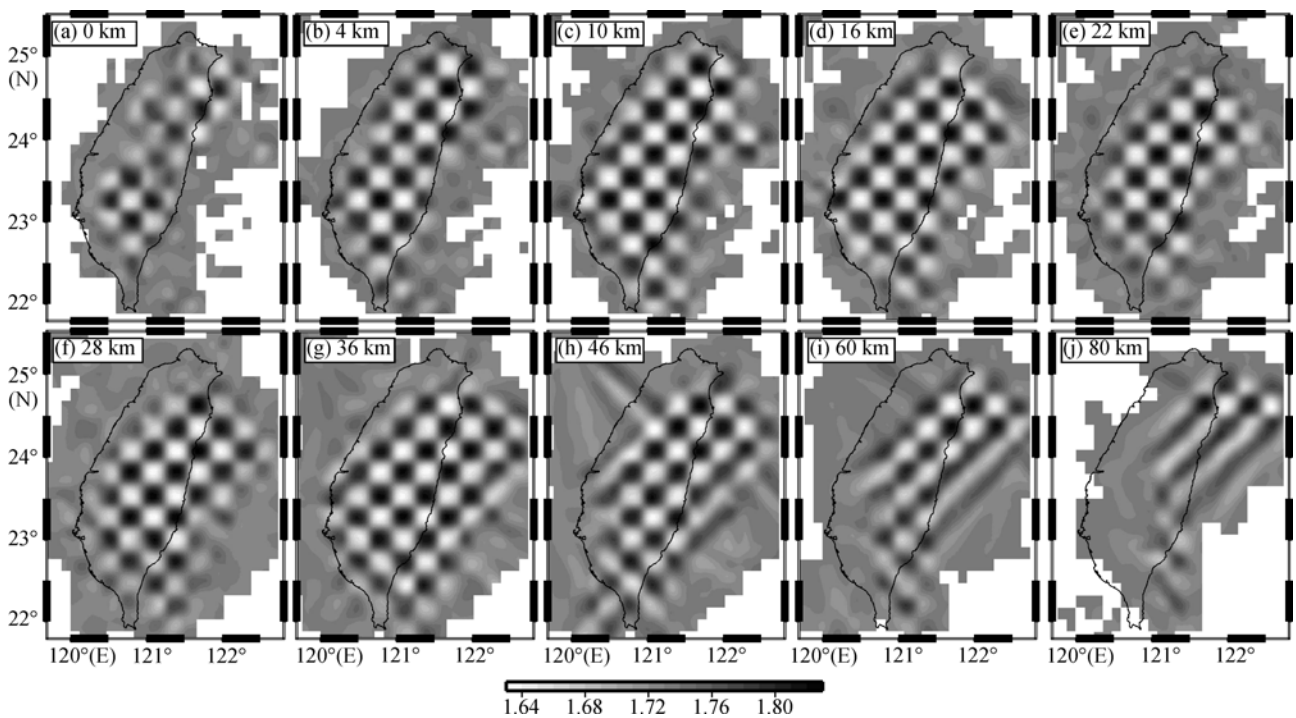

Figure 4 Recovered V_p/V_s models in checkerboard resolution tests at 0—80 km depth.

tures across the Taiwan orogen in EW and NS direction.

The low V_p and high V_p/V_s characters on profile A-A' (Figure 7(a)) at western Coastal Plain represent the thick sediments, contrasting against the high V_p and moderate low V_p/V_s anomalies in the middle-upper crust of the Central Range and Western Foothills. The earthquakes mainly occur on the east and west sides of the Central Range. Most of focal depths are less than 20 km beneath the western Coastal Plain, but reach 50—60 km beneath the Longitudinal Valley and Luzon Arc. The former ones

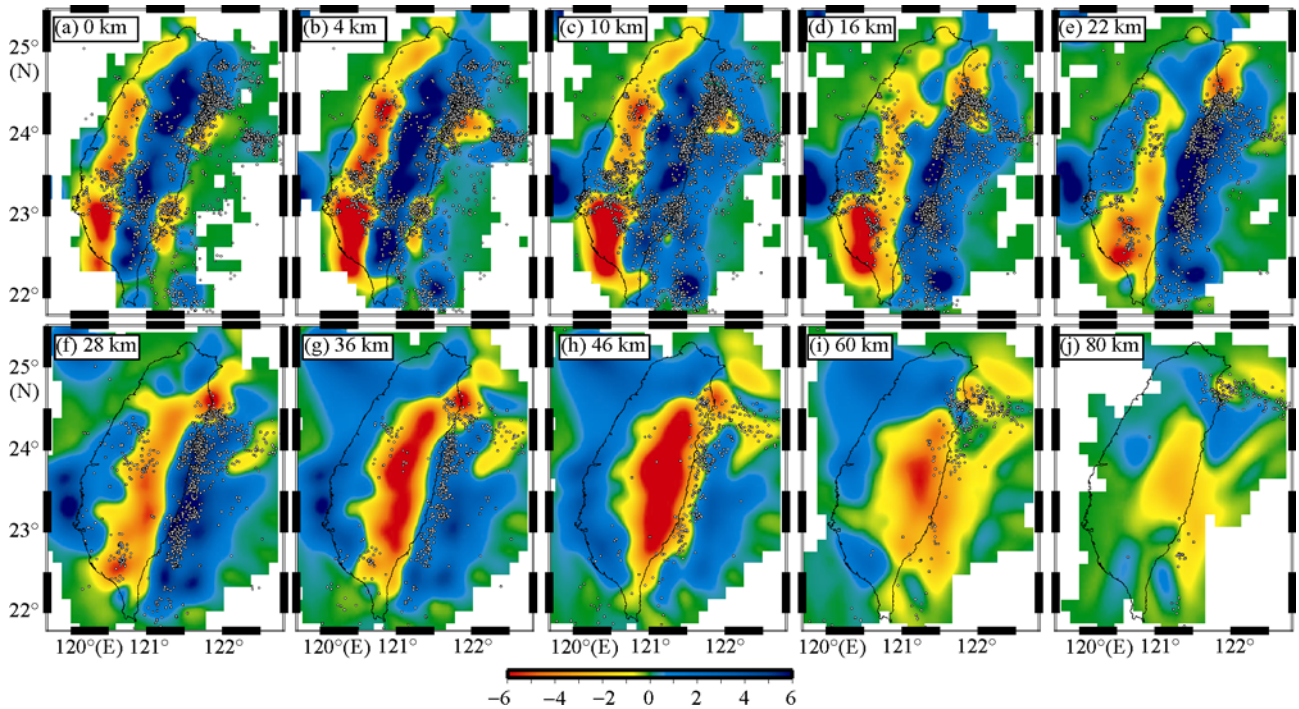

Figure 5 V_p perturbation maps (%) at 0—80 km depth. Open circles show the relocated events within ±10 km of each layer.

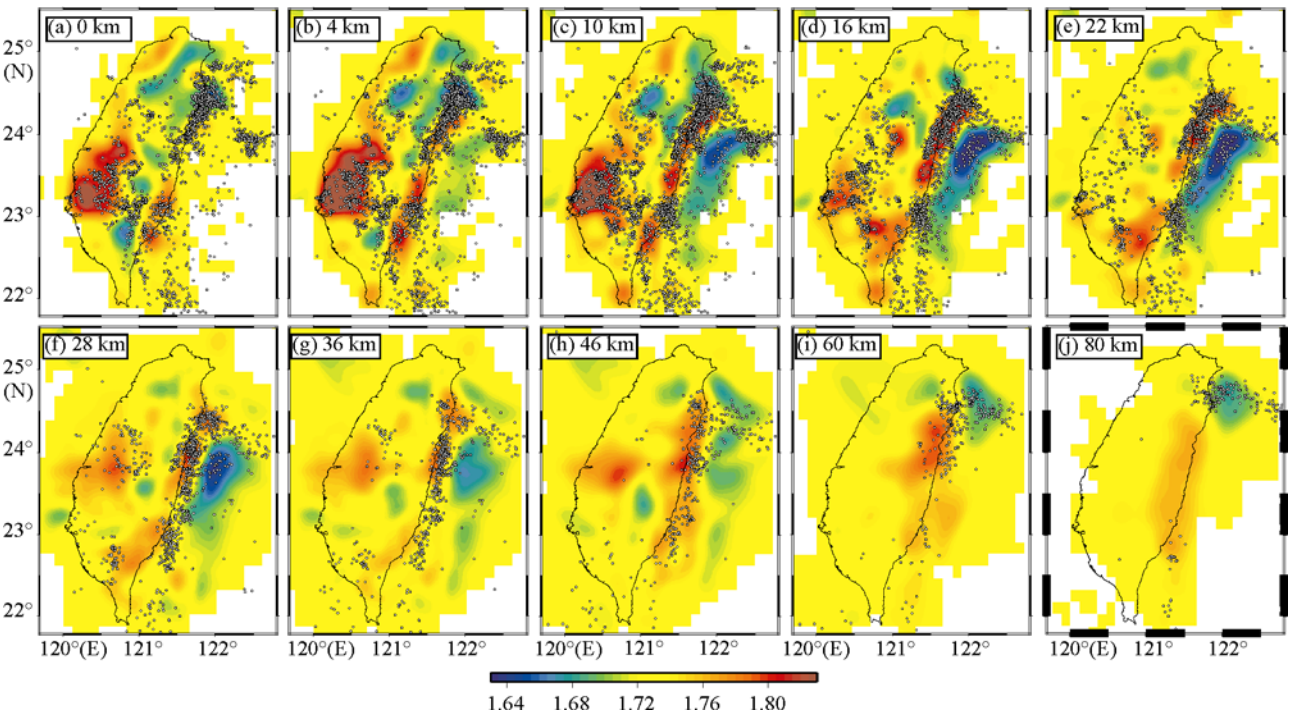

Figure 6 V_p/V_s distribution maps at 0—80 km depth. Open circles show the relocated events within ±10 km of each layer.

show the brittle rupture in the middle-upper crust, while the latter ones are obviously related to the collision of Eurasian Plate and Philippine Sea Plate. The V_p and V_p/V_s structures in these profiles suggest the prominent variations of the crust across Taiwan, and the crustal thickness reaches its maximum to the east of Central Range, which is coincident with the results from Rau et al.[4] and Kim et al.[5]. The fact that maximum crustal

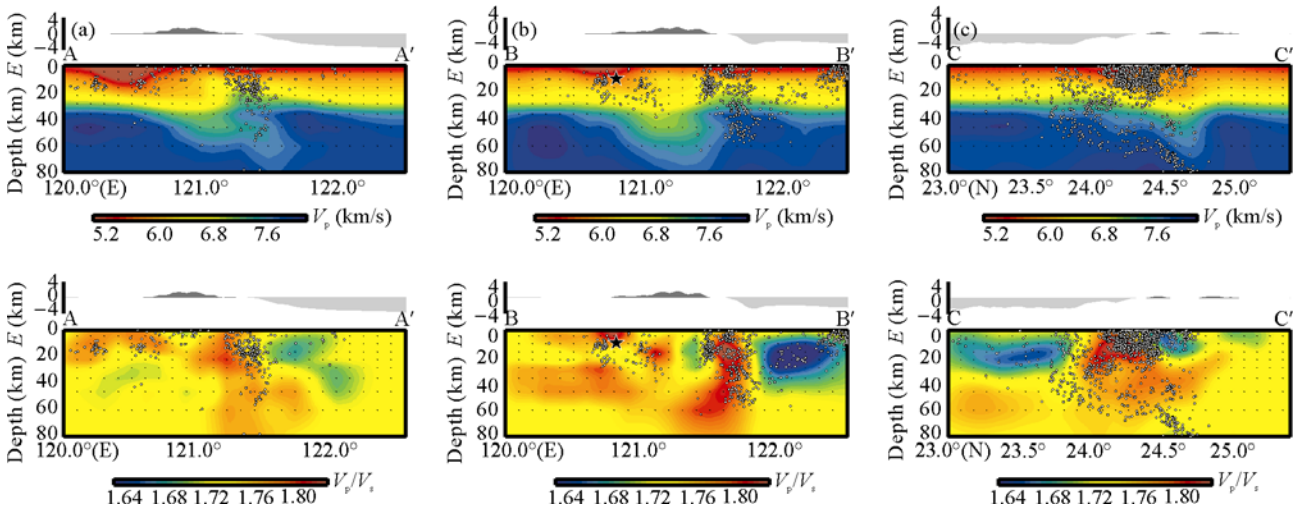

Figure 7 V_p and V_p/V_s ratio profiles. The locations of profiles are shown in Figure 2. Open circles show the relocated events within ±10 km of each profile, the black points show the grid node in the model, the pentagram on Figure 7(b) shows the position of M_w7.6 Chi-Chi earthquake on September 21, 1999. *E*, elevation.

thickness is not right beneath the Central Range and the deficiency of correlation between Bouguer gravity and topography suggest that the Taiwan area is not in isostatic equilibrium[5,27,28]. The focal mechanisms of moderate earthquakes indicate some amount of westward underthrusting at the Coastal Range, which suggests crustal thickening of the Philippine Sea Plate[9]. As the suture zone of the collision between Eurasian Plate and Philippine Sea Plate, the Longitudinal Valley has a large variation of crustal thickness, strong lateral contrast of V_p and V_p/V_s, and high seismicity. Most of the earthquakes occurred in the high V_p/V_s area and its boundary with the low V_p/V_s area (the high Poisson ratio area and its boundary with the low Poisson ratio area) and showed a trend of eastward dipping.

Profile B-B′ (Figure 7(b)) shows the similar V_p and V_p/V_s characters with profile A-A′, and reveals the velocity structures near the location of 1999 Chi-Chi earthquake (M_w=7.6). The earthquakes are mainly distributed on the two sides of Central Range; the ones near Taichung Basin show a low-angle eastward dipping trend, whereas the events on the western side of Central Range show a high-angle westward dipping trend. The seismicity is very low in the thickened middle-low crust beneath the Central Range[5]. The Chi-Chi earthquake is located in the transition zone between the low V_p, high V_p/V_s in the Taichung Basin and the high V_p, low V_p/V_s in the Western Foothills[29], which is coincident with the Chelungpu fault where the Western Foothills thrust westward onto the Taichung Basin at a low angle[30,31]. The earthquake activity reveals that the deformation due to the collision of Eurasian Plate and Philippine Sea Plate has already been transmitted to the west of Central Range[8]. In the area of Coastal Range and Luzon Arc, the high V_p/V_s (high Poisson ratio) signals and strong seismicity depict the fault system in the suture zone.

The V_p structure on profile C-C′ (Figure 7(c)) reveals the northward subducting Philippine Sea Plate, which is consistent with the north dipping seismicity down to 80 km depth. The low V_p and moderate high V_p/V_s anomalies are also coincident with the characters of other subduction zones[22]. As a developing back-arc basin, the Ilan Plain in north Taiwan is under extension in NS direction[4]. With the increase of depth, the accretion wedge derived from the crustal materials of subducting slab is characterized by high V_p/V_s anomaly, due to the presence of fluids from dehydration and increase of pore pressure[22]. Near the area of Hualien and Ilan, the large number of earthquakes in the upper to middle-lower crust, the presence of $M > 6$ normal-faulting earthquakes in the southwestern terminus of the Okinawa Trough off Ilan, the rapid subsidence of Ilan Plain, and the volcanic activities show the prominent tectonic activities of the back-arc basin in the northeast of Taiwan[4].

3 Conclusions

Combining P and S arrival time observations, we constructed the tomographic images of the V_p and V_p/V_s structures in the crust and upper mantle beneath the

Taiwan area using the spherical finite difference tomographic technique, and relocated the earthquakes with grid search approach. Our image of the crust and upper mantle is consistent with those determined in previous studies. The thickness of crust has large variations from west to the east, and reaches its maximum of 60 km beneath the east of Central Range. The deficiency of correlation between Bouguer gravity and elevation suggests that the Taiwan area is not in isostatic equilibrium and the mountain building is still ongoing. The low V_p and high V_p/V_s in the western Coastal Plain is related to the thick sediments and the presence of fluids in the upper crust. The Longitudinal Valley is the suture zone of Eurasian Plate and Philippine Sea Plate, and is also characterized by high V_p/V_s and strong seismicity, which could be due to the fault system, partial melting, and fluids incursion by the continent-arc collision. The configuration of the northward subducting Philippine Sea Plate along Ryukyu trench is very clear. The low V_p and high V_p/V_s anomalies near the Hualien and Ilan area could be due to the presence of fluids from dehydration of subducted slab and the increase of pore pressure, which is also coincident with the crustal structure with strong seismicity and volcanic activity.

We thank Prof. Liu Guangding for his direction, and Prof. Huang Zhongxian and the editors for their helps in improving this manuscript. Li Zhiwei wishes to thank Prof. S. Roecker from Rensselaer Polytechnic Institute for his enthusiastic encouragements and help. We appreciate the constructive reviews and comments of two anonymous reviewers, which improved the manuscript. This research is partially supported by China Scholarship Council.

1 Liu G D. Geophysical Series Maps in China Sea and Adjacent Regions. Beijing: Science Press, 1992
2 McIntosh K, Nakamura Y, Wang T K, et al. Crustal-scale seismic profiles across Taiwan and the western Philippine Sea. Tectonophysics, 2005, 401: 23－54[doi]
3 Li C F, Zhou Z Y, Li J B, et al. Precollisional tectonics and terrain amalgamation offshore southern Taiwan: Characterizations from reflection seismic and potential field data. Sci China Ser D-Earth Sci, 2007, 50(6): 897－908
4 Rau R, Wu F T, Tomographic imaging of lithospheric structures under Taiwan. Earth Planet Sci Lett, 1995, 133, 517－532[doi]
5 Kim K H, Chiu J M, Pujol J, et al. Three-dimensional V_p and V_s structural model associated with the active subduction and collision tectonics in the Taiwan region. Geophys J Int, 2005, 162, 204－220[doi]
6 Seno T, Stein S, Gripp A E. A model for the motion of the Philippine Sea Plate consistent with NUVEL-1 and geological data. J Geophys Res, 1993, 98:17941－17948[doi]
7 Yu S B, Chen H Y, Kou L C. Velocity field of GPS stations in the Taiwan area. Tectonophysics, 1997, 274:41－59[doi]
8 Bos A G, Spakman Nyst W, M C J. Surface deformation and tectonic setting of Taiwan inferred from a GPS velocity field. J Geophys Res, 2003, 108(B10): 2458[doi]
9 Wu F T, Rau R J, Salzberg D. Taiwan orogeny: Thin-skinned or lithospheric collision? Tectonophysics, 1997, 274: 191－220[doi]
10 Simoes M, Avouac J P, Beyssac O, et al. Mountain building in Taiwan: A thermokinematic model. J Geophys Res, 2007, 112: B11405, [doi]
11 Lallemand S, Font Y, Bijwaard H, et al. New insights on 3-D plates interaction near Taiwan from tomography and tectonic implications. Tectonophysics, 2001, 335: 229－253[doi]
12 Bautista B C, Bautista M L P, Oike K, et al. A new insight on the geometry of subducting slabs in northern Luzon, Philippines. Tectonophysics, 2001, 339: 279－310[doi]
13 Wang Z, Zhao D, Wang J, et al. Tomographic evidence for the Eurasian lithosphere subducting beneath south Taiwan. Geophys Res Lett, 2006, 33: L18306[doi]
14 Xu Y, Li Z W, Hao T Y, et al. Pn wave velocity and anisotropy in the northeastern South China Sea and adjacent region (in Chinese). Chin J Geophys, 2007, 50(5): 1473－1479
15 Huang B S, Huang W G, Liang W T, et al. Anisotropy beneath an active collision orogen of Taiwan: Results from across islands array observations. Geophys Res Lett, 2006, 33: L24302[doi]
16 Xu Y, Liu J H, Hao T Y, et al. P wave velocity structure and tectonic analysis of lithospheric mantle in eastern China seas and adjacent regions (in Chinese). Chin J Geophys, 2006, 49(4): 1053－1061
17 Roecker S W, Yeh Y H, Tsai Y B. Three-dimensional P and S wave velocity structures beneath Taiwan: Deep structure beneath and arc-continent collision. J Geophys Res, 1987, 92, 10547－10570[doi]
18 Wu Y M, Chang C H, Zhao L, et al. Seismic tomography of Taiwan: Improved constraints from a dense network of strong motion stations. J Geophys Res, 2007, 112: B08312[doi]
19 Li Z W, Roecker S. Tomographic imaging of the crust and upper mantle beneath the western Tien Shan. Eos Trans. AGU, 88(52), Fall Meet Suppl, Abstract 2007, T31B-0472
20 Li Z W. Seismic Tomography and the Crust and Upper Structure Beneath the Tien Shan (in Chinese). Dissertation for Doctoral Degree. Beijing: Graduate University of Chinese Academy of Sciences, 2008. 35－39
21 Eberhart-Phillips D. Three-dimensional P- and S-velocity structure in the Coalinga region, California. J Geophys Res, 1990, 95: 15343－15363[doi]
22 Eberhart-Phillips D, Reyners M, Chadwick M, et al. Crustal heterogeneity and subduction processes: 3-D V_p, V_p/V_s and Q in the southern North Island, New Zealand. Geophys J Int, 2005(162): 270－288

23 Reyners M, Eberhart-Phillips D, Stuart G. A three-dimensional image of shallow subduction: crustal structure of the Raukumara Peninsula, New Zealand. Geophys J Int, 1999, 137: 873－890[doi]
24 Roecker S, Thurber C, Roberts K, et al. Refining the image of the San Andreas Fault near Parkfield, California using a finite difference travel time computation technique. Tectonophysics, 2006, 426: 189－205[doi]
25 Paige C C, Saunders M A. LSQR: An algorithm for sparse linear equations and least squares problems. ACM Trans Math Software, 1982, 8: 43－71[doi]
26 Shyu J B, Sieh H K, Chen Y G, et al. Neotectonic architecture of Taiwan and its implications for future large earthquakes. J Geophys Res, 2005, 110: B08402[doi]
27 Wang W M, Yao Z X. A study on the 3D crustal structure beneath Taiwan by teleseismic transform function method (in Chinese). Chin J Geophy, 2003, 46(5): 628－632
28 Hwang C, Hsiao Y S, Shih H C, et al. Geodetic and geophysical results from a Taiwan airborne gravity survey: Data reduction and accuracy assessment. J Geophys Res, 2007, 112: B04407[doi]
29 Zhou S Y, Chen X F. Inversion of near-field waveform data for earthquake source rupture process(II): Inversion of Chi Chi earthquake source, 20 September, 1999, Taiwan. Sci China Ser D-Earth Sci, 2006, 49(3): 272－282
30 Lin C H, Ando M. Seismological evidence of simultaneous mountain-building and crust-thickening from the 1999 Taiwan Chi-Chi earthquake (M_w=7.6). Earth Planets Space, 2004, 56: 163－167
31 Lee S J, Chen H W, Ma K F. Strong ground motion simulation of the 1999 Chi-Chi, Taiwan earthquake from a realistic three-dimensional source and crustal structure. J Geophys Res, 2007, 112: B06307